V47

Molar Heat of Copper

Fritz Agildere
fritz.agildere@udo.edu

Amelie Strathmann
amelie.strathmann@udo.edu

Experiment: May 13, 2024
Submission: May 13, 2024

TU Dortmund – Department of Physics

Contents

1 Objective

By investigating the heat capacity of copper, we test some of the most prominent models for their validity and determine select characteristic quantities of solids.

2 Theory [1]

In the description of condensed matter, tools from classical thermodynamics and statistical physics as well as quantum mechanical considerations need to be applied. Throughout the following paragraphs, we explore some of the more well known models in the subfield of thermal properties, specifically for the explanation of the heat capacity in solids.

2.1 Heat Capacity

The heat capacity of any material is defined via

$$C \equiv \frac{\Delta Q}{\Delta T}$$

as the amount of heat ΔQ corresponding to a unit change ΔT in temperature. This is clearly dependent on the amount of matter, so to allow for comparisons between different materials we can normalize with volume V or mass M to obtain a specific heat capacity.

2.1.1 Molar Heat

In our case, we are interested in the heat capacity per number of particles making up a sample. This leads to

$$c \equiv \frac{\Delta Q}{n\Delta T}$$

for the molar heat capacity, where n is the number of mol contained in the substance. To determine n one can use readily available values of the molar mass m or molar volume v for the given experimental parameters.

2.1.2 Measurement

During the measuring process, it is necessary to constrain certain parameters. To grasp the following relations, we examine the first and second laws of thermodynamics

$$\mathrm{d}U = \delta Q - \delta W = T\mathrm{d}S - P\mathrm{d}V$$

where U is the internal energy, Q and W are heat and work, T stands for temperature, S for entropy, P for pressure and V for volume. The symbols d and δ denote exact and inexact differentials, respectively.

From this relation, we identify $\delta Q = T\mathrm{d}S$ and thereby

$$C = T\frac{\partial S}{\partial T}$$

when translating the defining statement to infinitesimal notation.

2.1.2.1 Isochoric Case

At fixed volume, all units of heat result in temperature changes exclusively. The isochoric heat capacity can be written as

$$C_V = T\left.\frac{\partial S}{\partial T}\right|_V$$

and constitutes an interesting quantity to study the behaviour of materials due to the isolation of otherwise connected effects.

2.1.2.2 Isobaric Case

When the pressure is kept constant instead, some of the heat exchange also results in expansion or contraction of the sample and therefore reduces the total temperature difference. Intuition therefore tells us that $C_P > C_V$ where we write

$$C_P = T\left.\frac{\partial S}{\partial T}\right|_P$$

for the isobaric heat capacity. This situation is more easily realizable in experiments but comes at the cost of no longer separating different mechanisms affecting the substance.

2.1.2.3 Connection

In order to convert between C_P and C_V we need some generally applicable relationship between the two quantities. We establish the differential form for entropy

$$\mathrm{d}S = \left.\frac{\partial S}{\partial T}\right|_V \mathrm{d}T + \left.\frac{\partial S}{\partial V}\right|_T \mathrm{d}V$$

in terms of volume as an extensive and temperature as an intensive property. We obtain

$$\left.\frac{\partial S}{\partial T}\right|_P = \left.\frac{\partial S}{\partial T}\right|_V + \left.\frac{\partial S}{\partial V}\right|_T \left.\frac{\partial V}{\partial T}\right|_P$$

by differentiating, allowing us to reformulate our desired quantites

$$C_P - C_V = T\left(\left.\frac{\partial S}{\partial T}\right|_P - \left.\frac{\partial S}{\partial T}\right|_V\right) = T\left.\frac{\partial S}{\partial V}\right|_T \left.\frac{\partial V}{\partial T}\right|_P$$

as the difference between them.

A combination of Jacobian coordinate transformations and Maxwell relations yields

$$C_P - C_V = \alpha_V^2 \kappa_T T V \tag{1}$$

with the isothermal bulk modulus

$$\kappa_T = -V \left. \frac{\partial P}{\partial V} \right|_T$$

and the volumetric thermal expansion coefficient

$$\alpha_V = \frac{1}{V} \left. \frac{\partial V}{\partial T} \right|_P$$

of the material. For isotropic materials, the last term is equivalent to the form $\alpha_V = 3\,\alpha_L$ via the linear analogue

$$\alpha_L = \frac{1}{L} \left. \frac{\partial L}{\partial T} \right|_P$$

which gives

$$C_P - C_V = 9\,\alpha_L^2\,\kappa_T T V$$

as the final expression. For typical solids with strong binding forces this difference is negligible, though it becomes more relevant for liquid or gaseous states of matter.

2.2 Models

All approaches discussed in this section model condensed matter as perfect crystal lattices with normal modes of participating members as purely harmonic oscillations. In the Hooke regime, the center of mass does not change with increasing or decreasing energy. Accordingly, the volume is constant under heat exchange and the condition $C_V = C_P$ is always fulfilled. This is of course unphysical, but it should serve as a decent approximation for the materials we are interested in. To account for thermal contraction, we would need to consider anharmonic effects by expanding the assumed potential minimum to higher orders.

2.2.1 Classical Physics

The equipartition theorem from classical thermodynamics affords a mean energy

$$\langle u \rangle = \frac{1}{2} k_B T$$

to each available degree of freedom. For a singular uncoupled harmonic oscillator, we have the spacial components of position and velocity as free coordinates. In this view, a three dimensional system of N atoms has an internal energy

$$U = 3Nk_BT = 3nRT$$

when we impose zero equilibrium potential. Here $R = N_A k_B$ is the universal gas constant, N_A is the Avogadro constant and k_B is the Boltzmann constant.

Because $\mathrm{d}V = 0$ and therefore $\mathrm{d}U = \delta Q$ we can simply write

$$C = \frac{\partial U}{\partial T} = 3Nk_B = 3nR$$

to find the heat capacity as predicted through the empirical law by Dulong and Petit.

2.2.2 Quantum Mechanics

The classical result estimates the heat capacity reasonably well for high temperatures. At lower temperatures however, we expect quantum mechanical effects to play a significant role. This is explained by the quantization of energy in multiples of $\hbar\omega$ dividing the range of allowed states into discrete levels. At temperatures where $k_B T \gg \hbar\omega$ the energy space appears continuous to thermal excitations whereas $k_B T \ll \hbar\omega$ forces most members to remain frozen in the ground state. To visualize this description, figure 1 presents a conceptual sketch.

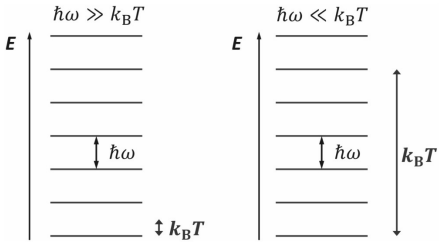

Figure 1: Exemplary energy discretization in low and high temperature limits. [1]

2.2.2.1 Phonons

As shown in figure 2 collective lattice vibrations show two types of dispersion relation.

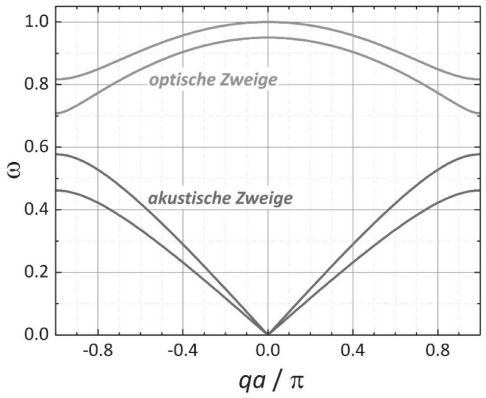

Figure 2: Schematic phonon branches inside the first Brillouin zone. [1]

Optical branches result from out of phase oscillations, where neighboring atoms have opposite velocity vectors. Conversely, acoustic branches represent in phase or parallel vibrational modes. For a crystal with k basis atoms, there are 3 acoustic and $3k-3$ optical dispersion curves. The differences between these solutions can be more or less relevant under different circumstances.

We call such quantized sound waves phonons, which funtion as quasiparticles with similar behaviour to photons as gauge bosons acting like quantized light waves. An important characteristic is the vanishing chemical potential μ indicating that population numbers are not conserved and that quasiparticles can be created or destroyed.

In accordance with the previous statement, the mean equilibrium population

$$\langle n \rangle = \frac{1}{e^{\beta\hbar\omega} - 1}$$

follows statistics as described by Bose and Einstein, where

$$\beta \equiv \frac{1}{k_B T}$$

is the thermodynamic beta and the exponentials trace back to Boltzmann weighting as well as the convergence of the geometric series. From the energy levels of a quantum harmonic oscillator

$$E_n = \hbar\omega \left(\frac{1}{2} + n\right)$$

we find the internal energy

$$U = \sum_{\boldsymbol{q}\,r} \frac{1}{2}\hbar\omega_{\boldsymbol{q}\,r} + \sum_{\boldsymbol{q}\,r} \frac{\hbar\omega_{\boldsymbol{q}\,r}}{e^{\beta\hbar\omega_{\boldsymbol{q}\,r}} - 1}$$

where we sum over all allowed reciprocal vectors $\boldsymbol{q}$ and polarisations r to account for multiatomic bases. The heat capacity follows as

$$C = \frac{\partial}{\partial T} \sum_{\boldsymbol{q}\,r} \frac{\hbar\omega_{\boldsymbol{q}\,r}}{e^{\beta\hbar\omega_{\boldsymbol{q}\,r}} - 1}$$

in the most general case. Due to $\sum_{\boldsymbol{q}\,r} = 3N$ we always get $C = 3Nk_B$ at high temperatures by expanding the exponential function to linear order. This asymptote reproduces the classical result as asserted by the correspondence principle independent from any further restrictions introduced by additional simplifications. The global models described below therefore both approach the same value at high thermal energies but differ when quantum effects dominate at low temperatures.

2.2.2.2 Einstein

The core assumption proposed by Einstein is a monochromatic eigenmode spectrum. By introducing ω_E as the frequency for all oscillations, we can write

$$C = \frac{\partial}{\partial T} \sum_{\boldsymbol{q}r} \frac{\hbar\omega_E}{e^{\beta\hbar\omega_E} - 1}$$

and after differentiating

$$C = 3N \frac{\hbar^2\omega_E^2}{k_B T^2} \frac{e^{\beta\hbar\omega_E}}{(e^{\beta\hbar\omega_E} - 1)^2}$$

with $\sum_{\boldsymbol{q}r} = 3N$ for the summation. We introduce the Einstein temperature

$$\vartheta_E \equiv \frac{\hbar\omega_E}{k_B}$$

and reformulate the previous expression as

$$C = 3Nk_B \left(\frac{\vartheta_E}{T}\right)^2 \frac{e^{\vartheta_E/T}}{(e^{\vartheta_E/T} - 1)^2}$$

for our result. By using the expansions $e^{\vartheta_E/T} = 1$ and $e^{\vartheta_E/T} - 1 = \vartheta_E/T$ it is trivial to show that $C = 3Nk_B$ at high temperatures. With $e^{\vartheta_E/T} \gg 1$ we find

$$C = 3Nk_B \left(\frac{\vartheta_E}{T}\right)^2 e^{-\vartheta_E/T}$$

in the low temperature limit. The flat dispersion underlying these results most closely resembles the typical behavior of optical phonons. Due to their contribution being most significant at higher energies, the accuracy of the cold regime approximation suffers as acoustic phonons dominate.

2.2.2.3 Debye

According to Debye, we replace all phonon branches with the three acoustic ones and approximate these to exhibit linear dispersion. Additionally, instead of summing over wave vectors $\boldsymbol{q}$ we integrate over a spherical constant energy surface of the first Brillouin zone. Each dispersion branch contains N states occupying a total phase space volume

$$8\pi^3 \frac{N}{V} = \frac{4}{3}\pi q_D^3$$

where the right hand side follows as the volume of a sphere with radius q_D equal to the magnitude of the reciprocal Debye vector.

Solving this equation leads to

$$q_D = \left(6\pi^2 \frac{N}{V}\right)^{1/3}$$

which defines $\omega_{D\,i} = q_D v_i$ for the frequencies. We see here that the speed of sound

$$v_i = \frac{\omega_{D\,i}}{q_D} = \frac{\partial \omega_{D\,i}}{\partial q_D}$$

is both the phase and group velocity. Accounting for the density of states, we find

$$C = \frac{\partial}{\partial T} \sum_{i=1}^{3} \int_0^{2\pi} \mathrm{d}\varphi \int_0^{\pi} \mathrm{d}\vartheta \sin\vartheta \int_0^{q_D} \mathrm{d}q\, q^2 Z(q)\, \frac{\hbar q v_i}{e^{\beta \hbar q v_i} - 1}$$

in spherical coordinates. We define the cubed harmonic mean sound velocity v_s via

$$\frac{1}{v_s^3} = \frac{1}{3} \sum_{i=1}^{3} \frac{1}{v_i^3}$$

or more explicitly

$$v_s = \left(\frac{1}{3v_l^3} + \frac{2}{3v_t^3}\right)^{-1/3}$$

where we require identical velocities v_t for both transversal components with the singular longitudinal mode v_l as independent. Using this, we can write

$$C = \frac{3V\hbar^2 v_s^2}{2\pi^2 k_B T^2} \int_0^{q_D} \mathrm{d}q\, \frac{q^4 e^{\beta \hbar q v_s}}{(e^{\beta \hbar q v_s} - 1)^2}$$

after integrating over the solid angle and differentiating with respect to temperature. The substitution $x \equiv \beta \hbar q v_s$ gives

$$C = \frac{3V k_B^4 T^3}{2\pi^2 \hbar^3 v_s^3} \int_0^{\beta \hbar q_D v_s} \mathrm{d}x\, \frac{x^4 e^x}{(e^x - 1)^2}$$

as an equivalent formulation. By introducing the Debye temperature

$$\vartheta_D \equiv \frac{\hbar \omega_D}{k_B} = \frac{\hbar q_D v_s}{k_B} = \frac{\hbar v_s}{B} \left(6\pi^2 \frac{N}{V}\right)^{1/3} \tag{2}$$

we finally arrive at

$$C = 9Nk_B \left(\frac{T}{\vartheta_D}\right)^3 \int_0^{\vartheta_D/T} \mathrm{d}x\, \frac{x^4 e^x}{(e^x - 1)^2}$$

for our result. At high temperatures $e^x = 1$ and $e^x - 1 = x$ lead to $C = 3Nk_B$ again.

In the case of low temperatures, the integral approaches

$$\int_0^\infty \mathrm{d}x \, \frac{x^4 e^x}{(e^x - 1)^2} = \frac{4\pi^4}{15}$$

and the heat capacity

$$C = \frac{12\pi^4}{5} N k_B \left(\frac{T}{\vartheta_D} \right)^3$$

has a cubic temperature dependence. Thanks to the assumption of linear dispersion, this closely matches observations. From the above considerations

$$\omega_D = q_D v_s = \left(18\pi^2 \left(\frac{1}{v_l^3} + \frac{2}{v_t^3} \right)^{-1} \frac{N}{V} \right)^{1/3} \tag{3}$$

gives the prescription for the resulting frequency.

2.2.2.4 Electrons

Especially in metals, the contribution from free electrons can add significantly to the heat capacity. We model this as an ideal fermion gas, meaning that all interactions are governed by the Pauli exclusion principle, resulting in a statistic as described by Fermi and Dirac. From a Sommerfeld expansion we find

$$C = \frac{\pi^2}{2} N k_B \frac{T}{T_F}$$

where the Fermi temperature T_F is defined via the Fermi energy $E_F = k_B T_F$ and the heat capacity depends linearly on the absolute temperature. Exemplary isochoric heat capacities can be viewed in figure 3 to compare the competing models.

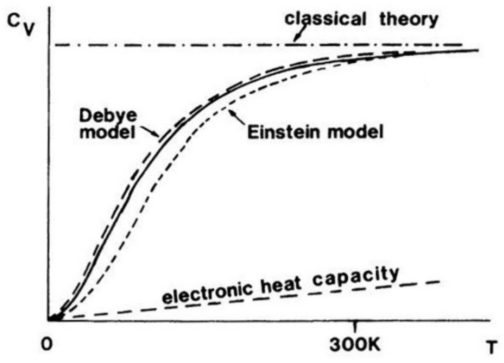

Figure 3: Different models of isochoric heat capacity for a typical solid material. [6]

3 Setup

The analysed copper sample is contained inside another copper cylinder with separate heating coils. For both parts, the temperature can be measured reliably using platinum thermistors, which exhibit a well defined monotonic resistance curve over broad ranges. These components are placed inside the recipient, which is connected to a vacuum pump and can be filled with helium at normal pressure. Surrounding this is a Dewar flask, meant to be filled with liquid nitrogen for cooling and isolating the entire apparatus. As an overview, figure 4 outlines the arranged equipment graphically.

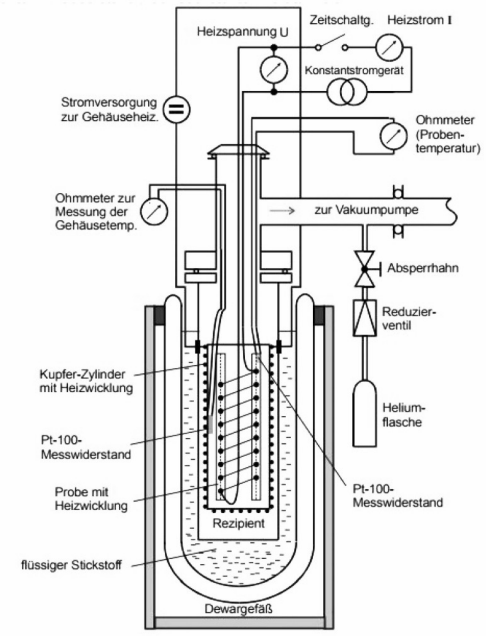

Figure 4: Schematic depiction of the measuring apparatus. [5]

4 Procedure

Initially, the sample needs to be cooled down. First, we evacuate the recipient and replace the air with helium gas. Due to its low boiling point of 4 K the new medium remains gaseous even at temperatures around 77 K where air might liquify and any water contents would freeze. This allows us to achieve lower pressures by again removing all gases from the recipient after the lowest temperature is reached in order to prevent heat losses via conduction, convection, evaporation or radiation. Now we proceed with taking actual measurements. To this end, sample and cylinder are supplied with heat energy via electrical power, minimizing the temperature gradient and thereby increasing accuracy. We record intervals of temperature ΔT and time Δt as well as voltage U and current I to determine $\Delta Q = UI\Delta t$ and from this the isobaric heat capacity. Finally, we convert to the isochoric case and discuss some important observations.

5 Results

In the following, the molar heat capacity and then the Debye temperature are determined.

5.1 Parameters

The copper sample in this experiment has a mass of $m = 0.342\,\mathrm{kg}$ [5] and a density of $\rho = 8930\,\mathrm{kg/m^3}$ [2]. Table 1 shows the molar volume and the compression modulus of copper.

Table 1: Parameters of the copper sample.

Parameter	Value
V_m	$7.11 \times 10^{-6}\,\mathrm{m^3/mol}$ [3]
κ	140 GPa [4]

The molar mass, the number of moles and the number of particles can then be calculated. The following applies to the molar mass

$$M = V_m \cdot \rho = 0.0634\,\mathrm{kg\,mol^{-1}}.$$

The number of moles is calculated as follows

$$n = \frac{m}{M} = 5.103$$

The result for the number of particles is

$$N = n \cdot N_A = 3.07 \times 10^{24}.$$

The volume of the sample is calculated as follows

$$V = \frac{m}{\rho} = 3.628 \times 10^{-5}\,\mathrm{m^3}.$$

The transverse velocity of sound and the longitudinal velocity of sound are also required for further calculations. These are $v_t = 2260\,\mathrm{m\,s^{-1}}$ and $v_l = 4700\,\mathrm{m\,s^{-1}}$ [5].

5.2 Theoretical Debye Temperature

The Debye temperature is calculated using formula 2. The Debye frequency is determined by formula 3. The result for the Debye temperature with the parameters given in section 5.1 is

$$\vartheta_D = 332.208\,\mathrm{K}.$$

5.3 Calculation of the Molar Heat Capacity Cp

The molar heat capacity C_P can be calculated using the equation

$$C_\mathrm{P} = \frac{1}{n} \cdot \frac{E}{\Delta T}. \tag{4}$$

Here the energy is defined as follows

$$E = I \cdot U \cdot \Delta t. \tag{5}$$

The calculated heat capacities are shown in Table 2.

Table 2: Temperature difference ΔT, time intervall Δt, voltage U, current I and the molar heat capacity C_P.

ΔT/K	Δt/s	U/V	I/mA	C_P/J K^{-1} mol^{-1}
11.87 ± 0.34	382.00 ± 7.07	17.20 ± 0.01	164.1	12.40 ± 7.57
10.02 ± 0.34	336.00 ± 7.07	17.37 ± 0.01	165.4	21.47 ± 13.00
10.07 ± 0.34	340.00 ± 7.07	17.45 ± 0.01	166.0	18.95 ± 11.44
9.87 ± 0.34	356.00 ± 7.07	17.52 ± 0.01	166.4	19.68 ± 11.85
9.92 ± 0.34	350.00 ± 7.07	17.57 ± 0.01	166.8	20.62 ± 12.39
9.96 ± 0.34	377.00 ± 7.07	17.61 ± 0.01	167.0	20.25 ± 12.15
10.01 ± 0.35	377.00 ± 7.07	17.64 ± 0.01	167.3	21.79 ± 13.05
10.05 ± 0.35	383.00 ± 7.07	17.67 ± 0.01	167.4	22.08 ± 13.22
10.10 ± 0.35	384.00 ± 7.07	17.69 ± 0.01	167.6	22.09 ± 13.21
10.14 ± 0.35	415.00 ± 7.07	17.71 ± 0.01	167.7	23.81 ± 14.23
9.69 ± 0.35	373.00 ± 7.07	17.72 ± 0.01	167.8	22.43 ± 13.40
9.98 ± 0.35	386.00 ± 7.07	17.73 ± 0.01	167.9	22.56 ± 13.47
10.02 ± 0.35	408.00 ± 7.07	17.74 ± 0.01	168.0	23.77 ± 14.18
9.81 ± 0.36	400.00 ± 7.07	17.75 ± 0.01	168.0	23.82 ± 14.21
10.11 ± 0.36	450.00 ± 7.07	17.75 ± 0.01	168.1	26.03 ± 15.52
9.90 ± 0.36	422.00 ± 7.07	17.76 ± 0.01	168.2	24.96 ± 14.87
10.19 ± 0.36	392.00 ± 7.07	17.76 ± 0.01	168.2	22.51 ± 13.41
9.98 ± 0.36	420.00 ± 7.07	17.76 ± 0.01	168.3	24.65 ± 14.68

5.4 Calculation of the Molar Heat Capacity C_V

The molar heat capacity C_V can be calculated using equation 1. The values of the expansion coefficient can be read from figure 7. The heat capacities, the temperatures and the expansion coefficient are shown in table 3.

Table 3: Tempearture T, heat capacity C_V and expansion coefficient α.

T/K	C_V/J K^{-1} mol^{-1}	α
91.44 ± 0.24	12.32 ± 7.57	9.75×10^{-6}
103.31 ± 0.24	21.36 ± 13.00	1.07×10^{-5}
113.33 ± 0.24	18.82 ± 11.44	1.15×10^{-5}
123.39 ± 0.24	19.52 ± 11.85	1.21×10^{-5}
133.27 ± 0.24	20.43 ± 12.39	1.265×10^{-5}
143.18 ± 0.24	20.03 ± 12.15	1.315×10^{-5}
153.15 ± 0.24	21.54 ± 13.05	1.36×10^{-5}
163.15 ± 0.24	21.81 ± 13.22	1.39×10^{-5}
173.21 ± 0.25	21.79 ± 13.21	1.425×10^{-5}
183.30 ± 0.25	23.48 ± 14.23	1.45×10^{-5}
193.45 ± 0.25	22.06 ± 13.40	1.475×10^{-5}
203.14 ± 0.25	22.16 ± 13.47	1.495×10^{-5}
213.12 ± 0.25	23.34 ± 14.18	1.52×10^{-5}
223.14 ± 0.25	23.35 ± 14.21	1.54×10^{-5}
232.95 ± 0.25	25.53 ± 15.52	1.56×10^{-5}
243.06 ± 0.25	24.43 ± 14.87	1.575×10^{-5}
252.96 ± 0.25	21.95 ± 13.41	1.59×10^{-5}
263.15 ± 0.26	24.05 ± 14.68	1.610×10^{-5}
273.13 ± 0.26	24.05 ± 14.68	1.625×10^{-5}

The calculated heat capacity values were plotted as a function of temperature in plot 5.

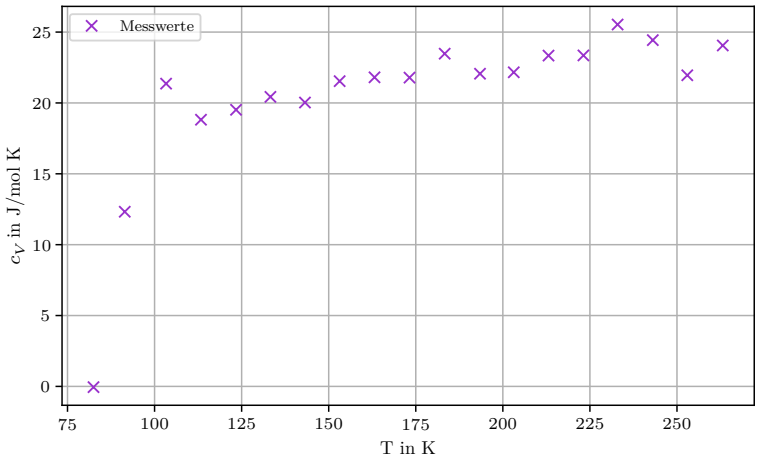

Figure 5: The molar heat capacity C_V as a function of temperature.

5.5 Experimental Debye Temperature

With the help of the table 8, the Debye temperature per temperature can be determined by reading the calculated values from our C_{V} and then assigning them. Then only the quotient $\frac{\vartheta_D}{T}$ has to be multiplied by the temperature T to obtain the Debye temperature ϑ_D. Values can only be calculated for temperatures below 170 K.

The calculated Debye temperatures are shown in Table 4.

Table 4: Temperature T, Debye temperature ϑ_D.

T/K	ϑ_D/K
91.44 ± 0.24	338.1 ± 1.0
103.31 ± 0.24	258.3 ± 0.6
113.33 ± 0.24	260.7 ± 0.5
123.39 ± 0.24	246.8 ± 0.5
133.27 ± 0.24	293.2 ± 0.5
143.18 ± 0.24	386.6 ± 0.7
153.15 ± 0.24	413.5 ± 0.7
163.15 ± 0.24	440.5 ± 0.7

The mean value of the Debye temperatures is (299.27 ± 0.19) K.

6 Discussion

The experimental value for the Debye temperature is $\vartheta_{\mathrm{exp}} = (299.27 \pm 0.19)$ K. The theoretical Debye temperature is calculated to be $\vartheta_{\mathrm{theo}} = 332.208$ K. From this follows a relative deviation of the experimental value by 9.91%. The deviation is within the acceptable range, as systematic errors may have occurred during the experiment. First, heat convection can never be ruled out entirely, which could have influenced the measurement. Second, the sample was not completely insulated, which could have led to heat losses.

The theoretical molar heat capacity of copper is $C_{\mathrm{theo}} = 24.76\,\mathrm{J\,mol^{-1}\,K^{-1}}$ at room temperature [2]. The experimental value is $C_{\mathrm{exp}} = (24 \pm 15)\,\mathrm{J\,mol^{-1}\,K^{-1}}$ at a temperature of $T = (273.13 \pm 0.26)$ K. This closely matches the expectation with an uncertainty of 6%. The error could have arisen from the same factors as the Debye temperature.

The asymptotic progression of the heat capacity for high temperatures can be recognized in graph 5.

In summary, it can be said that the error calculation produces large uncertainties in the values.

Overall, the evaluation of the test was successful and the experimental values can be accepted with the given caveats.

References

[1] Rudolf Gross and Achim Marx. *Festkörperphysik*. Berlin, Boston: De Gruyter Oldenbourg, 2022. ISBN: 9783110782394. DOI: doi:10.1515/9783110782394. URL: https://doi.org/10.1515/9783110782394.

[2] *Kupfer. Eigenschaften*. Kupferverband e.V. 2024. URL: https://kupfer.de/kupferwerkstoffe/kupfer/eigenschaften/.

[3] *Kupfer*. Chemie.de. 2024. URL: https://www.chemie.de/lexikon/Kupfer.html.

[4] *Kupfer*. Periodensystem.info. 2024. URL: https://www.periodensystem-online.de/index.php?id=modify&el=29.

[5] *Manual for Experiment 47, Molar Heat of Copper*. TU Dortmund, Department of Physics. 2024.

[6] *Thermal Properties of Materials*. what-when-how. 2024. URL: https://what-when-how.com/electronic-properties-of-materials/thermal-properties-of-materials/.

Appendix

T[°C]	-200	-190	-180	-170	-160	-150	-140	-130	-120
R[Ω]	18,44	22,71	27,03	31,28	35,48	39,65	43,80	47,93	52,04
T[°C]	-110	-100	-90	-80	-70	-60	-50	-40	-30
R[Ω]	56,13	60,20	64,25	68,28	72,29	76,28	80,25	84,21	88,17
T[°C]	-20	-10	0	+10	+20	+30	+40		
R[Ω]	92,13	96,07	100	103,90	107,79	111,67	115,54		

Figure 6: Resistance to temperature conversion table. [5]

T [K]	70	80	90	100	110	120	130	140
α [10^{-6} grd^{-1}]	7,00	8,50	9,75	10,70	11,50	12,10	12,65	13,15
T [K]	150	160	170	180	190	200	210	220
α [10^{-6} grd^{-1}]	13,60	13,90	14,25	14,50	14,75	14,95	15,20	15,40
T [K]	230	240	250	260	270	280	290	300
α [10^{-6} grd^{-1}]	15,60	15,75	15,90	16,10	16,25	16,35	16,50	16,65

Figure 7: Temperature to linear thermal expansion coefficient conversion table. [5]

θ_D/T	0	1	2	3	4	5	6	7	8	9
0	24,9430	24,9310	24,8930	24,8310	24,7450	24,6340	24,5000	24,3430	24,1630	23,9610
1	23,7390	23,4970	23,2360	22,9560	22,6600	22,3480	22,0210	21,6800	21,3270	20,9630
2	20,5880	20,2050	19,8140	19,4160	19,0120	18,6040	18,1920	17,7780	17,3630	16,9470
3	16,5310	16,1170	15,7040	15,2940	14,8870	14,4840	14,0860	13,6930	13,3050	12,9230
4	12,5480	12,1790	11,8170	11,4620	11,1150	10,7750	10,4440	10,1190	9,8030	9,4950
5	9,1950	8,9030	8,6190	8,3420	8,0740	7,8140	7,5610	7,3160	7,0780	6,8480
6	6,6250	6,4090	6,2000	5,9980	5,8030	5,6140	5,4310	5,2550	5,0840	4,9195
7	4,7606	4,6071	4,4590	4,3160	4,1781	4,0450	3,9166	3,7927	3,6732	3,5580
8	3,4468	3,3396	3,2362	3,1365	3,0403	2,9476	2,8581	2,7718	2,6886	2,6083
9	2,5309	2,4562	2,3841	2,3146	2,2475	2,1828	2,1203	2,0599	2,0017	1,9455
10	1,8912	1,8388	1,7882	1,7393	1,6920	1,6464	1,6022	1,5596	1,5184	1,4785
11	1,4400	1,4027	1,3667	1,3318	1,2980	1,2654	1,2337	1,2031	1,1735	1,1448
12	1,1170	1,0900	1,0639	1,0386	1,0141	0,9903	0,9672	0,9449	0,9232	0,9021
13	0,8817	0,8618	0,8426	0,8239	0,8058	0,7881	0,7710	0,7544	0,7382	0,7225
14	0,7072	0,6923	0,6779	0,6638	0,6502	0,6368	0,6239	0,6113	0,5990	0,5871
15	0,5755	0,5641	0,5531	0,5424	0,5319	0,5210	0,5117	0,5020	0,4926	0,4834

Figure 8: Debye temperature ratio conversion table. [5]

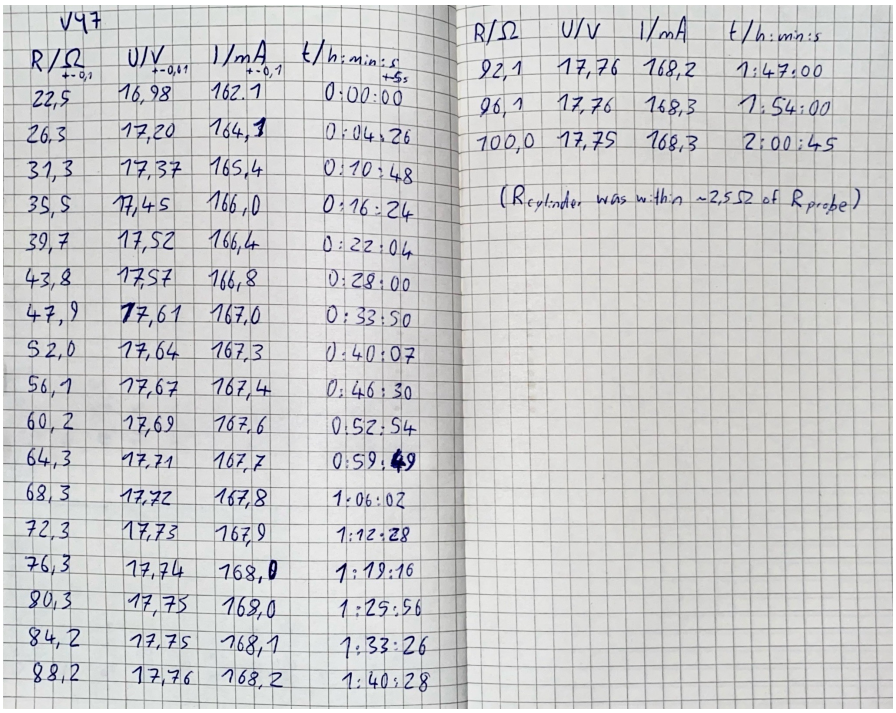

V47

R/Ω ±0,1	U/V ±0,01	I/mA ±0,1	t/h:min:s ±5s
22,5	16,98	162,1	0:00:00
26,3	17,20	164,1	0:04:26
31,3	17,37	165,4	0:10:48
35,5	17,45	166,0	0:16:24
39,7	17,52	166,4	0:22:04
43,8	17,57	166,8	0:28:00
47,9	17,61	167,0	0:33:50
52,0	17,64	167,3	0:40:07
56,1	17,67	167,4	0:46:30
60,2	17,69	167,6	0:52:54
64,3	17,71	167,7	0:59:49
68,3	17,72	167,8	1:06:02
72,3	17,73	167,9	1:12:28
76,3	17,74	168,0	1:19:16
80,3	17,75	168,0	1:25:56
84,2	17,75	168,1	1:33:26
88,2	17,76	168,2	1:40:28

R/Ω	U/V	I/mA	t/h:min:s
92,1	17,76	168,2	1:47:00
96,1	17,76	168,3	1:54:00
100,0	17,75	168,3	2:00:45

($R_{cylinder}$ was within ~2,5Ω of R_{probe})

Figure 9: Original handwritten measurements.